CrossMark
click for updates

Hydrophilic–hydrophobic phase transition of photoresponsive linear and macrocyclic poly(2-isopropyl-2-oxazoline)s†

Yongseok Jung, Jaehyuk Nam, Joo-Ho Kim and Woo-Dong Jang*

A series of macrocyclic and linear poly(2-isopropyl oxazoline)s containing a photoresponsive azobenzene moiety (**Az-PiPOx**s) were synthesized by Cu(I)-catalyzed cycloaddition reaction between azide-functionalized azobenzene and alkyne-bearing poly(2-isopropyl oxazoline)s. Upon temperature elevation, both macrocyclic and linear **Az-PiPOx** exhibited a sharp hydrophilic-to-hydrophobic phase transition: the initially clear solution became turbid at specific temperatures. The photoisomerization of the azobenzene moiety resulted in the large change of the thermal transition temperature of the polymers. *cis* isomers exhibited a higher thermal transition temperature than *trans* isomers. Thus, the phase transition can be controlled by 365 and 254 nm UV irradiation.

Introduction

Stimuli-responsive polymers that change their properties according to external environment provide a great opportunity for the development of functional materials.[1–4] Various types of stimuli-responsive polymers have been exploited for the design of functional materials such as biological interfaces, drug delivery systems, and logic gates.[2,5–8] Poly(2-isopropyl-2-oxazoline) (**PiPOx**) is a well-known thermoresponsive polymer that exhibits hydrophilic–hydrophobic thermal transition *via* the lower critical solution temperature.[9] Because **PiPOx**s have a lower critical solution temperature, around human body temperature, and excellent biocompatibility, they have been receiving significant attention for biomedical applications.[10–13] Macrocyclic polymers (*i.e.*, polymers with a closed topology) have no chain ends,[14] and the structural uniqueness endows them with properties distinguishable from those of linear polymers. Namely, macrocyclic polymers have smaller hydrodynamic volume, lower solution viscosity, higher thermal stability, and higher glass transition temperature as compared to linear polymers of similar molecular weight.[15–17] Moreover, macrocyclic polymers often show improved chemical stability due to the absence of chain ends,[18] and the closed topology offers additional advantages for their application in the biomedical field.[19–22] For example, Grayson *et al.* reported a cyclic poly(ethylene imine) (PEI) as a carrier for *in vitro* gene transfection, which exhibited higher transfection efficacy and lower cytotoxicity than linear PEI.[20] In addition, some macrocyclic polymers

displayed longer circulation times than linear polymers. Such unique properties of macrocyclic polymers are highly beneficial for drug delivery and other biomedical applications.[23] However, because of their synthetic difficulty, macrocyclic polymers have not been sufficiently investigated. Ring-closure reactions between the end groups of linear polymers are frequently used for the synthesis of macrocyclic polymers;[24,25] namely, the click reaction between azide and alkyne groups, which affords a triazole heterocycle in high yields and under very mild conditions,[26,27] proved to be very useful.[28–32] In this study, we have synthesized dual stimuli-responsive macrocyclic **PiPOx**s *via* click chemistry. Clickable **PiPOx**s ending with alkyne groups have been prepared *via* cationic ring-opening polymerization of oxazoline monomers.[33–37] The click reaction with azobenzene derivatives having two azide groups afforded macrocyclic **PiPOx**s with a photoresponsive azobenzene group in the macrocyclic ring. The dual stimuli-responsive properties of the macrocyclic **PiPOx** were compared with those of the linear **PiPOx**.

Experimental section

Materials and measurements

All commercially available reagents were reagent grade and used without further purification. Dichloromethane, *N,N*-dimethylformamide (DMF), carbon tetrachloride, tetrahydrofuran (THF), and acetonitrile were freshly distilled before each use. Recycling preparative size-exclusion chromatography (SEC) was performed on a LC-9201 (JAI, Tokyo, Japan) instrument equipped with JAIGEL-1H, JAIGEL-2H, and JAIGEL-3H columns using CHCl₃ as the eluent. Electronic absorption spectra were measured using a V-660 (JASCO, Tokyo, Japan) spectrophotometer equipped with a thermostatic cell holder coupled with a controller (ETCS-761, JASCO, Tokyo, Japan). ¹H NMR spectra

Department of Chemistry, Yonsei University, 50 Yonsei-ro, Seodaemun-gu, Seoul 03722, Korea. E-mail: wdjang@yonsei.ac.kr

† Electronic supplementary information (ESI) available: NMR, MALDI-TOF-MS and IR spectra, SEI profiles. See DOI: 10.1039/c7ra01042g

were recorded using a Bruker DPX 400 (400 MHz) spectrometer in CDCl$_3$ or CD$_2$Cl$_2$. Analytical SEC was performed on a JASCO HPLC equipped with HF-403HQ and HF-404HQ columns (Shodex, Tokyo, Japan) using THF as the eluent. Matrix-assisted laser desorption ionization time-of-flight mass spectrometry (MALDI-TOF-MS) measurements were performed on a Bruker model LRF20 using dithranol (1,8,9-trihydroxyanthracene) as the matrix. FT-IR spectra were recorded on Bruker Vertex 70 FT-IR spectrometer. UV irradiation experiments were performed using a UV hand lamp (Vilber Lourmat, France) equipped with 4 W UV discharge tubes. For the UV irradiation, quartz cells or NMR tubes were placed at a distance of 5 mm from the lamp.

Determination of thermal transition temperature

The transmittance of the solution at 800 nm was measured using a spectrophotometer. The heating rate of the sample cells was adjusted to 1.0 °C min^{-1}. The thermal transition temperature was taken as the temperature at which the transmittance reached 50% in the resulting transmittance *versus* temperature curves.

Synthesis

The synthetic routes to azobenzene-containing linear and cyclic poly(2-isopropyl-2-oxazoline)s (l-**Az-PiPOx** and c-**Az-PiPOx**, respectively) are outlined in Scheme 1. 4,4′-Bis(azidomethyl) azobenzene and 2-isopropyl-2-oxazoline (**iPOx**) were synthesized according to literature procedures.[38–40]

General procedures for polymerization reaction. A Schlenk flask was degassed under high vacuum and backfilled with N$_2$; this process was repeated three times. A solution of initiator (propargyl *p*-toluenesulfonate or methyl *p*-toluenesulfonate) in acetonitrile was placed in the Schlenk flask, and **iPOx** was added to it. The mixture solution was stirred at 40 °C under N$_2$ atmosphere and the reaction was monitored by analytical SEC and MALDI-TOF-MS. Upon completion of the reaction, *N*-methylpropargylamine was poured into the reaction mixture, and then further stirred for 24 h. The solution of **PiPOx** was purified *via* dialysis for 2 days against distilled water and then recovered by lyophilisation.
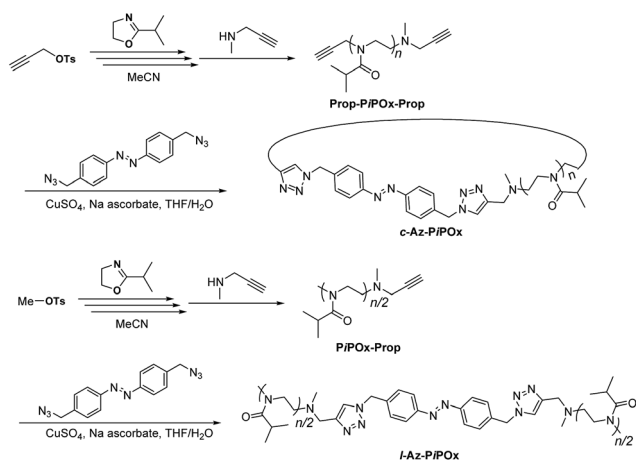
Scheme 1 Synthesis of l-**Az-PiPOx** and c-**Az-PiPOx**.

Prop-PiPOx$_{2k}$-Prop. 1.27 g of propargyl *p*-toluenesulfonate (1.04 mL, 6.02 mmol), 11.4 g of **iPOx** (12.0 mL, 100.7 mmol) and 0.835 g of *N*-methylpropargylamine (1.02 mL, 12.08 mmol) in acetonitrile (15.0 mL) were used to prepare **Prop-PiPOx$_{2k}$-Prop** as white powder (7.8 g, 68%). ^{1}H NMR (400 MHz, CD$_2$Cl$_2$, 25 °C) δ (ppm): 4.23–4.12 (m; initiation terminal N–CH$_2$–C≡), 3.48–3.42 (broad d; –CH$_2$–CH$_2$– on the polymer backbone), 2.88–2.60 (broad t; –CH– on the polymer side chain, α-terminal –C≡CH, ω-terminal –N–CH$_2$–C≡CH), 2.33 (broad s; terminal –N–CH$_3$), 1.06 (strong broad s; –CH– on the polymer side chain).

Prop-PiPOx$_{4k}$-Prop. 0.79 g of propargyl *p*-toluenesulfonate (0.65 mL, 3.76 mmol), 14.3 g of **iPOx** (15.0 mL, 126.4 mmol) and 0.401 g of *N*-methylpropargylamine (0.49 mL, 5.80 mmol) in acetonitrile (20 mL) were used to prepare **Prop-PiPOx$_{4k}$-Prop** as white powder (12.3 g, 86%). ^{1}H NMR (400 MHz, CD$_2$Cl$_2$, 25 °C) δ (ppm): 4.24–4.13 (m; initiation terminal N–CH$_2$–C≡), 3.50–3.43 (broad d; –CH$_2$–CH$_2$– on the polymer backbone), 2.89–2.69 (broad t; –CH– on the polymer side chain, α-terminal –C≡CH, ω-terminal –N–CH$_2$–C≡CH), 2.32 (broad s; terminal –N–CH$_3$), 1.08 (strong broad s; –CH– on the polymer side chain).

PiPOx$_{1k}$-Prop. 1.93 g of methyl *p*-toluenesulfonate (1.56 mL, 10.36 mmol), 9.5 g of **iPOx** (10.0 mL, 83.9 mmol) and 1.43 g of *N*-methylpropargylamine (1.75 mL, 20.7 mmol) in acetonitrile (12.5 mL) were used to prepare **PiPOx$_{1k}$-Prop** mixture solution. The solution was concentrated under reduced pressure and 2.0 g of residue was purified by recycling preparative SEC using CHCl$_3$ as the eluent. After purification, 1.4 g of **PiPOx$_{1k}$-Prop** was recovered as a white powder upon lyophilisation (yield = 70%). ^{1}H NMR (400 MHz, CD$_2$Cl$_2$, 25 °C) δ (ppm): 3.50–3.43 (broad d; –CH$_2$–CH$_2$– on the polymer backbone), 3.04 (broad s; terminal N–CH$_3$), 2.90–2.55 (broad m; –CH– on the polymer side chain, terminal –N–CH$_2$–C≡CH), 2.32 (broad s; terminal –N–CH$_3$), 1.08 (strong broad s; –CH– on the polymer side chain).

PiPOx$_{2k}$-Prop. 0.55 g of propargyl *p*-toluenesulfonate (0.45 mL, 2.97 mmol), 5.7 g of **iPOx** (6.0 mL, 50.4 mmol) and 0.246 g of *N*-methylpropargylamine (0.30 mL, 3.6 mmol) in acetonitrile (9.0 mL) were used to prepare **PiPOx$_{2k}$-Prop** as white powder (4.2 g, 74%). ^{1}H NMR (400 MHz, CD$_2$Cl$_2$, 25 °C) δ (ppm): 3.50–3.43 (broad d; –CH$_2$–CH$_2$– on the polymer backbone), 3.04 (broad s; terminal N–CH$_3$), 2.90–2.59 (broad m; –CH– on the polymer side chain, terminal –N–CH$_2$–C≡CH), 2.32 (broad s; terminal –N–CH$_3$), 1.08 (strong broad s; –CH– on the polymer side chain).

General procedure for the click reaction. A mixture of 4,4′-bis(azidomethyl)azobenzene, **PiPOx**, and copper(II) sulfate in THF was placed in a round-bottom flask. Sodium ascorbate was dissolved in H$_2$O and poured into the reaction mixture. The mixture was refluxed for 2 days, and then the solution was cooled to room temperature and poured into dichloromethane. The organic layer was washed several times with brine and dried over anhydrous Na$_2$SO$_4$. The combined organic layers were concentrated under reduced pressure. And then the residue was purified by recycling preparative SEC using CHCl$_3$ as the eluent, and lyophilized.

c-Az-PiPOx$_{2k}$. 500.0 mg of **Prop-PiPOx$_{2k}$-Prop** (0.25 mmol), 74.5 mg of 4,4′-bis(azidomethyl)azobenzene (0.26 mmol),

399.0 mg of copper(II) sulfate (2.5 mmol), 495.3 mg of sodium ascorbate (2.5 mmol), and 600 mL of THF/H₂O (99/1) were used to afford c-**Az-PiPOx**$_{2k}$ as a bright orange powder (160 mg, 32%). ^{1}H NMR (400 MHz, CD₂Cl₂, 25 °C) δ (ppm): 7.92–6.82 (m; N–CH=N in the triazole ring, –CH on the azobenzene group), 5.61 (s; N–CH₂–C between the triazole ring and the azobenzene group), 4.60 (broad s; N–CH₂–C beside the triazole ring), 3.69 (broad s; N–CH₂–C opposite side of the triazole ring), 3.47–3.41 (broad d; –CH₂–CH₂– on the polymer backbone), 2.88–2.50 (broad m; –CH– on the polymer side chain), 2.26 (broad s; terminal –N–CH₃), 1.06 (strong broad s; –CH– on the polymer side chain).

c-Az-PiPOx$_{4k}$. 500.0 mg of **Prop-PiPOx**$_{4k}$**-Prop** (0.13 mmol), 37.3 mg of 4,4′-bis(azidomethyl)azobenzene (0.13 mmol), 199.5 mg of copper(II) sulfate (1.3 mmol), 247.6 mg of sodium ascorbate (2.5 mmol), and 600 mL of THF/H₂O (99/1) were used to afford c-**Az-PiPOx**$_{4k}$ as a bright orange powder (160 mg, 32%). ^{1}H NMR (400 MHz, CD₂Cl₂, 25 °C) δ (ppm): 8.01–6.81 (m; N–CH=N in the triazole ring, –CH on the azobenzene group), 5.61 (s; N–CH₂–C between the triazole ring and the azobenzene group), 4.61 (broad s; N–CH₂–C beside the triazole ring), 3.70 (broad s; N–CH₂–C opposite side of the triazole ring), 3.49–3.43 (broad d; –CH₂–CH₂– on the polymer backbone), 2.89–2.51 (broad m; –CH– on the polymer side chain), 2.27 (broad s; terminal –N–CH₃), 1.07 (strong broad s; –CH– on the polymer side chain).

l-Az-PiPOx$_{2k}$. 500 mg of **PiPOx**$_{1k}$**-Prop** (0.5 mmol), 73.1 mg of 4,4′-bis(azidomethyl)azobenzene (0.25 mmol), 399.0 mg of copper(II) sulfate (2.5 mmol), 495.3 mg of sodium ascorbate (2.5 mmol), and 60 mL of THF/H₂O (9/1) were used to afford l-**Az-PiPOx**$_{2k}$ as a bright orange powder (210 mg, 42%). ^{1}H NMR (400 MHz, CD₂Cl₂, 25 °C) δ (ppm): 7.92–6.83 (m; N–CH=N in the triazole ring, –CH on the azobenzene group), 5.60 (s; N–CH₂–C between the triazole ring and the azobenzene), 3.70 (broad s; N–CH₂–C beside the triazole ring), 3.49–3.42 (broad d; –CH₂–CH₂– on the polymer backbone), 3.04 (broad s; terminal N–CH₃), 2.90–2.53 (broad m; –CH– on the polymer side chain), 2.27 (broad s; terminal –N–CH₃), 1.07 (strong broad s; –CH– on the polymer side chain).

l-Az-PiPOx$_{4k}$. 500 mg of **PiPOx**$_{2k}$**-Prop** (0.5 mmol), 36.5 mg of 4,4′-bis(azidomethyl)azobenzene (0.125 mmol), 399.0 mg of copper(II) sulfate (2.5 mmol), 495.3 mg of sodium ascorbate (2.5 mmol), and 60 mL of THF/H₂O (9/1) were used to afford l-**Az-PiPOx**$_{4k}$ as a bright orange powder (205 mg, 41%). ^{1}H NMR (400 MHz, CD₂Cl₂, 25 °C) δ (ppm): 7.92–6.83 (m; N–CH=N in the triazole ring, –CH on the azobenzene group), 5.60 (s; N–CH₂–C between the triazole ring and the azobenzene), 3.70 (broad s; N–CH₂–C beside the triazole ring), 3.49–3.43 (broad d; –CH₂–CH₂– on the polymer backbone), 3.07 (broad s; terminal N–CH₃), 2.90–2.52 (broad m; –CH– on the polymer side chain), 2.27 (broad s; terminal –N–CH₃), 1.08 (strong broad s; –CH– on the polymer side chain).

Results and discussion

Synthesis and characterization

The synthetic routes to l-**Az-PiPOx**s and c-**Az-PiPOx**s are summarized in Scheme 1. Firstly, propargyl-bearing telechelic

PiPOxs (**Prop-PiPOx-Prop**) were prepared for the synthesis of c-**Az-PiPOx**s. In order to introduce propargyl groups at both initiation and termination ends, propargyl *p*-toluenesulfonate and *N*-methylpropargylamine were used as the initiator and terminating agent, respectively. The ratio of initiator to monomer was adjusted to be 1 : 17 and 1 : 34 to obtain **Prop-PiPOx-Prop** with number average molecular weights (M_n) approximately 2.0 and 4.0 kDa, respectively. For the synthesis of l-**Az-PiPOx**s, the propargyl group was introduced only at the termination end. Methyl *p*-toluenesulfonate and *N*-methylpropargylamine were used as the initiator and terminating agent, respectively, to afford **PiPOx-Prop**. In order to obtain l-**Az-PiPOx**s with M_n similar to that of c-**Az-PiPOx**s, the initiator to monomer ratio was adjusted to 1 : 8 or 1 : 17. Next, the Cu(I)-catalysed cycloaddition (click reaction) between the propargyl groups in **Prop-PiPOx-Prop** and **PiPOx-Prop** and the azide groups in 4,4′-bis(azidomethyl)azobenzene were performed to obtain l-**Az-PiPOx**s and c-**Az-PiPOx**s, respectively. To minimize the formation of dimeric or trimeric compounds, the synthesis of c-**Az-PiPOx**s was performed under diluted conditions. It should be noted that l-**Az-PiPOx**s and c-**Az-PiPOx**s were purified by recycling preparative SEC to remove dimeric and trimeric compounds as well as low molecular weight impurities.

The synthesized **Az-PiPOx**s were characterized by ^{1}HNMR, MALDI-TOF-MS, and FT-IR measurements. The ^{1}HNMR spectra of both c-**Az-PiPOx**s and l-**Az-PiPOx**s showed the proton signals of the azobenzene groups at 7.9–6.8 ppm, indicating the successful incorporation of the azobenzene units into the **PiPOx** chains through the click reaction. The ^{1}HNMR spectra suggested that the azobenzene groups were predominantly in the *trans* configuration (Fig. 1 and S5†).

The absolute molecular weights of **Az-PiPOx**s were measured by MALDI-TOF-MS analysis (Fig. 2 and S8†). In both cases of c-**Az-PiPOx**s and l-**Az-PiPOx**s, a series of peaks at approximately 113.16 Da intervals was observed, and the obtained *m/z* values showed less than 0.1% deviation from the calculated values. The M_n obtained form MALDI-TOF-MS ($M_{n\text{-MS}}$) of c-**Az-PiPOx**$_{2k}$, l-**Az-PiPOx**$_{2k}$, c-**Az-PiPOx**$_{4k}$, and l-**Az-PiPOx**$_{4k}$ were estimated to be 4.18, 4.04, 2.72 and 2.79 kDa, respectively.
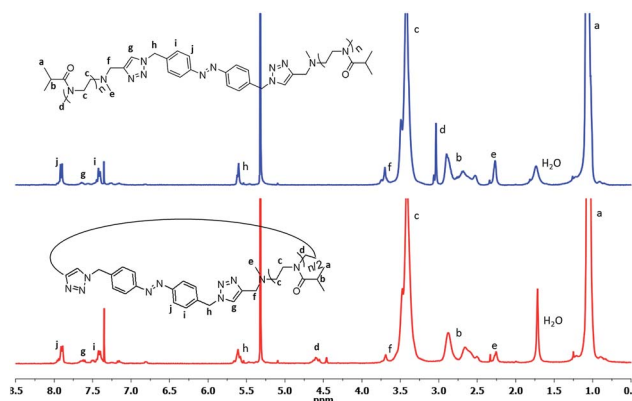

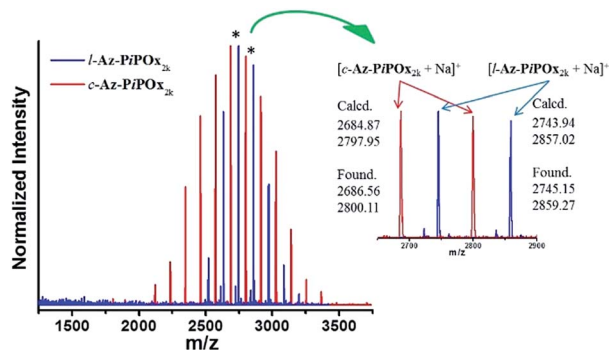**Fig. 1** ^{1}H NMR spectra of c-**Az-PiPOx**$_{2k}$ (top) and l-**Az-PiPOx**$_{2k}$ (bottom) in CD₂Cl₂.

Fig. 2 MALDI-TOF-MS spectra of c-**Az-PiPOx**$_{2k}$ (red line) and l-**Az-PiPOx**$_{2k}$ (blue line).

Fig. 4 SEC traces of l-**Az-PiPOx**$_{2k}$ (blue line) and c-**Az-PiPOx**$_{2k}$ (red line).

FT-IR measurements were performed to monitor the cyclo-addition reaction between 4,4′-bis(azidomethyl)azobenzene and the terminal alkyne groups of **PiPOx**s. As shown in Fig. 3, the FT-IR spectrum of 4,4′-bis(azidomethyl)azobenzene displays a sharp absorption peak at 2090 cm^{-1}, which originates from the azide groups. This peak completely disappeared upon formation of c-**Az-PiPOx**$_{2k}$ and l-**Az-PiPOx**$_{2k}$, indicating complete conversion during the cycloaddition reaction. The same aspect was observed for c-**Az-PiPOx**$_{4k}$ and l-**Az-PiPOx**$_{4k}$ (Fig. S9†).

Analytical SEC was performed for **Az-PiPOx**s (Fig. 4 and S12†) to estimate M_n values ($M_{n\text{-sec}}$) and dispersity indices ($Đ$). The retention peaks of c-**Az-PiPOx**$_{2k}$, l-**Az-PiPOx**$_{2k}$, c-**Az-PiPOx**$_{4k}$, and l-**Az-PiPOx**$_{4k}$ were appeared at 20.43, 20.65, 21.20 and 20.85 min, respectively. The $M_{n\text{-sec}}$ values of c-**Az-PiPOx**$_{2k}$, l-**Az-PiPOx**$_{2k}$, c-**Az-PiPOx**$_{4k}$, and l-**Az-PiPOx**$_{4k}$ were estimated to be 1.84, 2.53, 3.29, and 3.71 kDa, respectively, based on polystyrene standards. It is noteworthy that the $M_{n\text{-sec}}$ values of l-**Az-PiPOx**$_{2k}$ and l-**Az-PiPOx**$_{4k}$ were only 260 and 330 Da deviated from the $M_{n\text{-MS}}$ values of them, whereas the $M_{n\text{-sec}}$ values of c-**Az-PiPOx**$_{2k}$ and c-**Az-PiPOx**$_{4k}$ were much smaller than the $M_{n\text{-MS}}$ values of them (Table 1). In the SEC experiment, the retention time depends on the hydrodynamic volume of the polymer molecules. Generally, the hydrodynamic volume of macrocyclic polymers is smaller than that of linear polymers with equivalent molecular weight. Thus, the large differences of $M_{n\text{-sec}}$ values between c-**Az-PiPOx**s and l-**Az-PiPOx**s would be another evidence of macrocycle formation. Because the polymerization of **iPOx** proceeded through a living mechanism, **PiPOx-Prop** and **Prop-PiPOx-Prop**
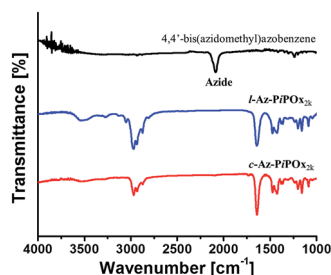
showed very narrow molecular weight distributions. After the click reaction with 4,4′-bis(azidomethyl)azobenzene, the resulting c-**Az-PiPOx**$_{2k}$, l-**Az-PiPOx**$_{2k}$, c-**Az-PiPOx**$_{4k}$, and l-**Az-PiPOx**$_{4k}$ were exhibited $Đ$ values of 1.06, 1.06, 1.07, and 1.09. In the preparation procedure of **Az-PiPOx**s, by-products and unreacted polymers were removed by recycling preparative SEC. Hence, very narrow molecular weight distributions could be obtained for both l-**Az-PiPOx**s and c-**Az-PiPOx**s.

Photoisomerization of the azobenzene moiety

In order to monitor the photoisomerization of the azobenzene moiety, a solution of c-**Az-PiPOx**$_{2k}$ in phosphate buffer (10 mM PBS and 150 mM NaCl, pH 7.4) was prepared and its change in UV-Vis absorption upon UV irradiation was measured. Upon 365 nm UV irradiation, the absorption spectrum of the c-**Az-PiPOx**$_{2k}$ solution (0.2 g L^{-1}) showed a gradual decrease of the peak at 329 nm and an increase of the band at 263 and 432 nm with clear isosbestic points at 282 and 390 nm (Fig. 5a), indicating *trans*-to-*cis* photoisomerization of the azobenzene moiety. The spectral shift was saturated after 15 min of 365 nm irradiation. Opposite changes were observed after 5 min of 254 nm UV irradiation (Fig. 5b). The *cis*-to-*trans* photoisomerization was faster than the *trans*-to-*cis* photoisomerization, presumably because the *trans* configuration is more stable. In order to confirm the reversibility of the

Fig. 3 FT-IR spectra of 4,4′-bis(azidomethyl)azobenzene, l-**Az-PiPOx**$_{2k}$ and c-**Az-PiPOx**$_{2k}$.

Table 1 The measured number average molecular weight (M_n) and $Đ$ (dispersity) for **PiPOx**s

		SEC^b		MS^c		
	$M_{n,\text{theo}}{}^a$	M_n	$Đ$	M_n	$Đ$	DP^c
PiPOx$_{1k}$**-Prop**	1000	1020	1.12	1180	1.02	10
PiPOx$_{2k}$**-Prop**	2000	2050	1.07	1990	1.01	17
Prop-PiPOx$_{2k}$**-Prop**	2000	2540	1.09	2240	1.01	20
Prop-PiPOx$_{4k}$**-Prop**	4000	4550	1.06	3890	1.01	34
l-**Az-PiPOx**$_{2k}$	2290	2530	1.07	2790	1.00	22
c-**Az-PiPOx**$_{2k}$	2290	1840	1.06	2720	1.01	21
l-**Az-PiPOx**$_{4k}$	4290	3710	1.09	4040	1.01	31
c-**Az-PiPOx**$_{4k}$	4290	3290	1.07	4180	1.01	33

^{a} Determined from the initiator/monomer ratio and the degree of conversion. ^{b} Determined by SEC analysis in THF using polystyrene standard. ^{c} Determined by MALDI-TOF-MS analysis.
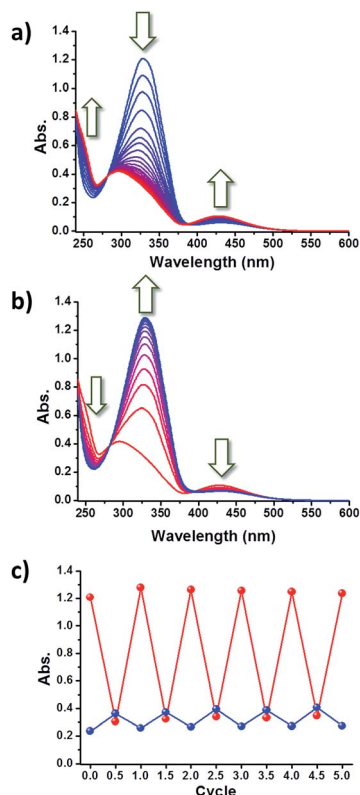
Fig. 5 UV-Vis absorption spectral changes of c-**Az-PiPOx**$_{2k}$ in 10 mM PBS (0.2 g L^{-1}) upon (a) 365 and (b) 254 nm irradiation. (c) Absorbance changes at 263 (blue) and 329 nm (red) upon 365 and 254 nm irradiation for 5 cycles.

Fig. 6 ^{1}HNMR spectra of 4,4′-bis(azidomethyl)azobenzene in the trans (a) and cis (b) configuration, and of c-**Az-PiPOx**$_{2k}$ in the trans (c) and cis configuration (d), in CD$_2$Cl$_2$. The peaks under the blue and red circles are attributed to the trans and cis forms of the azobenzene moieties, respectively.

photoisomerization, this experiment was repeated five times: as shown in Fig. 5c, the photoisomerization of the azobenzene moiety in c-**Az-PiPOx**$_{2k}$ was fully reversible under 365 and 254 nm UV irradiation.

The photoisomerization of c-**Az-PiPOx**$_{2k}$ and 4,4′-bis(azidomethyl)azobenzene was monitored by ^{1}H NMR spectroscopy. Solutions of c-**Az-PiPOx**$_{2k}$ and 4,4′-bis(azidomethyl)azobenzene in CD$_2$Cl$_2$ were irradiated with 365 nm UV light for 2 h to reach steady state conditions, and the ^{1}H NMR spectra were recorded (Fig. 6). The cis ratio of c-**Az-PiPOx**$_{2k}$ was estimated to be slightly lower (80%) than that of 4,4′-bis(azidomethyl)azobenzene (89%).

Thermoresponsiveness of Az-PiPOxs

The thermal transition temperatures of **Az-PiPOx**s were determined by temperature-dependent transmittance measurements. The transmittance of the solutions at 800 nm was monitored during temperature elevation of 1 °C min^{-1} rate, and the thermal transition temperatures were defined as the temperature at which 50% of the transmittance change occurred. Fig. 7 shows temperature-dependent transmittance changes of c-**Az-PiPOx**s and l-**Az-PiPOx**s at the concentration of 2.0 g L^{-1}. The thermal transition temperatures of l-**Az-PiPOx**$_{2k}$, c-**Az-PiPOx**$_{2k}$, l-**Az-PiPOx**$_{4k}$ and c-**Az-PiPOx**$_{4k}$ were determined to be 39.4, 33.8, 39.9 and 35.5 °C, respectively. It is well known that the thermal transition temperature of **PiPOx** decreases by
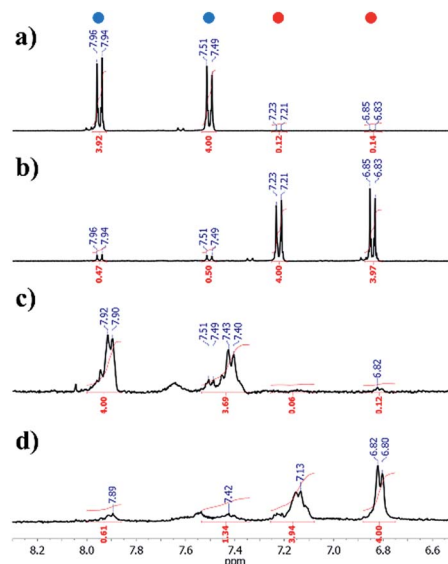
increasing molecular weight. As expected, **Az-PiPOx**$_{2k}$s show higher thermal transition temperature than **Az-PiPOx**$_{4k}$s. On the other hand, the thermal transition temperatures of l-**Az-PiPOx**s were higher than those of c-**Az-PiPOx**s. Because the chemical structures of l-**Az-PiPOx**s and c-**Az-PiPOx**s are not identical, the direct comparison of thermal transition temperatures may not be greatly meaningful. However, the
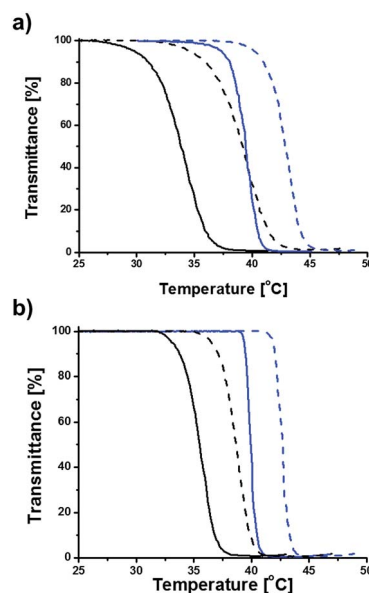

Fig. 7 Temperature dependent transmittance changes of (a) **Az-PiPOx**$_{2k}$s and (b) **Az-PiPOx**$_{4k}$s. Black and blue lines are corresponding to c-**Az-PiPOx**s and l-**Az-PiPOx**s, respectively. Solid and dashed lines are corresponding to trans and cis configurations of each polymers, respectively.

absence of chain terminals in c-**Az-PiPOx**s may influence on hydrophilicity of total polymers. When compared the optical transmittance change curves, l-**Az-PiPOx**s showed sharper transition than c-**Az-PiPOx**s. Such aspect has been reported previously in several poly(*N*-isopropyl acrylamide)-based systems.[30,41] It has been expected that the cyclic topology of thermoresponsive polymers can be affected the phase transition by the existence of repulsive force to prohibit intermolecular aggregation and steric constraints to induce intramolecular chain interactions.

To examine concentration dependency of thermal transition temperature, solutions of each **Az-PiPOx**s with concentration of 4.0, 2.0, 1.0 and 0.5 g L^{-1} in 10 mM PBS (NaCl 150 mM, pH 7.4) were prepared and optical transmittance changes were recorded. As increasing concentration of all **Az-PiPOx**s, the thermal transition temperatures were gradually decreased. Fig. 8 shows concentration dependent thermal transition temperature changes of **Az-PiPOx**s. All **Az-PiPOx**s showed linear correlation between thermal transition temperatures and logarithmic concentration. The steepness of slopes were varied by molecular weight and molecular topology. The slopes of **Az-PiPOx$_{2k}$**s were steeper than those of **Az-PiPOx$_{4k}$**s, indicating that lower molecular weight polymers have greater concentration dependency. On the other hand, the slopes of c-**Az-PiPOx**s were steeper than those of l-**Az-PiPOx**s, indicating cyclic polymers have higher concentration dependency than linear polymers.

The azobenzene moieties of l-**Az-PiPOx**s and c-**Az-PiPOx**s were photoisomerized to the *cis* form by 365 nm UV irradiation. After saturation of the photoisomerization, the thermal transition temperatures of l-**Az-PiPOx$_{2k}$**, c-**Az-PiPOx$_{2k}$**, l-**Az-PiPOx$_{4k}$**,

and c-**Az-PiPOx$_{4k}$** at 2.0 g L^{-1} were increased about 42.9, 39.1, 42.7 and 38.6 °C, respectively (Fig. 7 and 8). This observation can be explained by the polarization and morphological change of the azobenzene moiety: *cis*-azobenzene has a higher polarity than the *trans* isomer because the lone pair electrons are constrained to be on the same side. One of the unique aspects of the thermoresponsiveness of l-**Az-PiPOx**s and c-**Az-PiPOx**s is the difference in thermal transition temperature between *trans* and *cis* isomers. In our previous study, an increase in thermal transition temperature of only 0.9 °C was observed upon *trans*-to-*cis* photoisomerization of a **PiPOx** polymer with azobenzene moieties at the α and ω terminal ends.[5] In contrast, in this work, the *cis* and *trans* forms of both l-**Az-PiPOx**s and c-**Az-PiPOx**s exhibited significantly different thermal transition temperatures, where the differences of l-**Az-PiPOx$_{2k}$**, c-**Az-PiPOx$_{2k}$**, l-**Az-PiPOx$_{4k}$**, and c-**Az-PiPOx$_{4k}$** were 3.5, 5.3, 3.8, and 3.1 °C, respectively. This unique property can be attributed to morphological changes of the polymers by photoisomerization. In our previous study, the photoisomerization of the azobenzene moieties cannot induce morphological changes of whole of polymer because the azobenzene moieties are located at the terminal ends of the polymeric structure. In contrast, the morphologies of l-**Az-PiPOx**s and c-**Az-PiPOx**s can be drastically changed because the photoisomerizable unit located in the middle of polymer chains. Moreover, the morphological aspect of c-**Az-PiPOx**s would be greatly influenced by the photoisomerization due to the closed topology.

The large change in thermal transition temperature would be very useful for the design of thermo- and photo-responsive materials. Namely, **Az-PiPOx**s are highly attractive for application in the biomedical field because its thermal transition proceeds near the body temperature body temperature. As an example, we measured the phase transition of c-**Az-PiPOx$_{2k}$** at 2.0 g L^{-1} concentration at body temperature. The solution of *trans*-c-**Az-PiPOx$_{2k}$** became turbid when the temperature was raised to 36 °C. Under these conditions, the solution was continuously irradiated with 365 nm UV light and became transparent as a result of the *trans*-to-*cis* photoisomerization process (Fig. 9). Alternatively, the clear solution became turbid by continuous irradiation with 254 nm UV light. Thus, the hydrophilic–hydrophobic transition of **Az-PiPOx**s could be successfully controlled by photoirradiation.
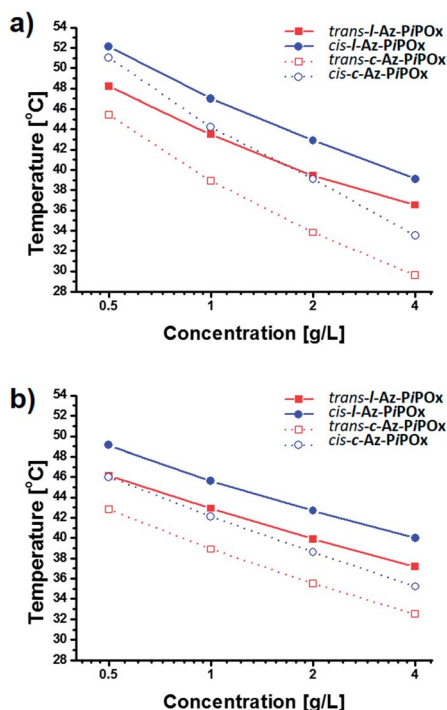

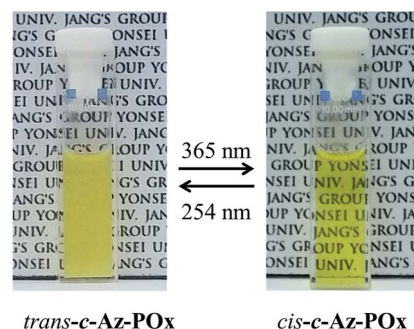Fig. 8 Concentration dependent thermal transition temperature changes of (a) **Az-PiPOx$_{2k}$**s and (b) **Az-PiPOx$_{4k}$**s.

Fig. 9 Turbidity change of c-**Az-PiPOx$_{2k}$** at 36 °C by UV irradiation.

Conclusions

In summary, dual stimuli-responsive linear and macrocyclic poly(2-isopropyl oxazoline) polymers containing a photo-responsive azobenzene group were prepared *via* living cationic polymerization followed by click reaction. In each polymer, the azobenzene moiety exhibited photoisomerization upon UV irradiation, and hydrophilic–hydrophobic phase transition was achieved upon temperature elevation. The photoisomerization of the azobenzene moiety resulted in the change of the thermal transition temperature of the polymers. *cis* isomers exhibited a higher thermal transition temperature than *trans* isomers. Thus, the phase transition can be controlled by 365 and 254 nm UV irradiation. Such unique property would make it an attractive material for various applications.

Acknowledgements

Notes and references

1 Y. Shen, X. Fu, W. Fu and Z. Li, *Chem. Soc. Rev.*, 2015, **44**, 612–622.

2 M. A. C. Stuart, W. T. Huck, J. Genzer, M. Müller, C. Ober, M. Stamm, G. B. Sukhorukov, I. Szleifer, V. V. Tsukruk and M. Urban, *Nat. Mater.*, 2010, **9**, 101–113.

3 F. D. Jochum and P. Theato, *Chem. Soc. Rev.*, 2013, **42**, 7468–7483.

4 J. H. Kim, Y. Jung, D. Lee and W. D. Jang, *Adv. Mater.*, 2016, **28**, 3499–3503.

5 J.-H. Kim, E. Koo, S.-Y. Ju and W.-D. Jang, *Macromolecules*, 2015, **48**, 4951–4956.

6 C. de las Heras Alarcón, S. Pennadam and C. Alexander, *Chem. Soc. Rev.*, 2005, **34**, 276–285.

7 F. D. Jochum, F. R. Forst and P. Theato, *Macromol. Rapid Commun.*, 2010, **31**, 1456–1461.

8 S. Masuda, T. Shimizu, M. Yamato and T. Okano, *Adv. Drug Delivery Rev.*, 2008, **60**, 277–285.

9 H. Uyama and S. Kobayashi, *Chem. Lett.*, 1992, 1643–1646.

10 A. L. Demirel, M. Meyer and H. Schlaad, *Angew. Chem., Int. Ed.*, 2007, **46**, 8622–8624.

11 R. Hoogenboom, *Angew. Chem., Int. Ed.*, 2009, **48**, 7978–7994.

12 R. Victor, *J. Mater. Sci.: Mater. Med.*, 2014, **25**, 1211–1225.

13 J. Zhao, R. Hoogenboom, G. Van Assche and B. Van Mele, *Macromolecules*, 2010, **43**, 6853–6860.

14 Z. Jia and M. J. Monteiro, *J. Polym. Sci., Part A: Polym. Chem.*, 2012, **50**, 2085–2097.

15 H. R. Kricheldorf, *J. Polym. Sci., Part A: Polym. Chem.*, 2010, **48**, 251–284.

16 X. Zhu, N. Zhou, Z. Zhang, B. Sun, Y. Yang, J. Zhu and X. Zhu, *Angew. Chem., Int. Ed.*, 2011, **50**, 6615–6618.

17 K. Endo, in *New Frontiers in Polymer Synthesis*, Springer, 2008, pp. 121–183.

18 M. Trabi and D. J. Craik, *Trends Biochem. Sci.*, 2002, **27**, 132–138.

19 H. Wei, D. S. Chu, J. Zhao, J. A. Pahang and S. H. Pun, *ACS Macro Lett.*, 2013, **2**, 1047–1050.

20 M. A. Cortez, W. T. Godbey, Y. Fang, M. E. Payne, B. J. Cafferty, K. A. Kosakowska and S. M. Grayson, *J. Am. Chem. Soc.*, 2015, **137**, 6541–6549.

21 N. Nasongkla, B. Chen, N. Macaraeg, M. E. Fox, J. M. Fréchet and F. C. Szoka, *J. Am. Chem. Soc.*, 2009, **131**, 3842–3843.

22 X. Y. Tu, M. Z. Liu and H. Wei, *J. Polym. Sci., Part A: Polym. Chem.*, 2016, **54**, 1447–1458.

23 B. Chen, K. Jerger, J. M. Fréchet and F. C. Szoka, *J. Controlled Release*, 2009, **140**, 203–209.

24 K. Pangilinan and R. Advincula, *Polym. Int.*, 2014, **63**, 803–813.

25 B. A. Laurent and S. M. Grayson, *Chem. Soc. Rev.*, 2009, **38**, 2202–2213.

26 J. E. Hein and V. V. Fokin, *Chem. Soc. Rev.*, 2010, **39**, 1302–1315.

27 H. C. Kolb, M. Finn and K. B. Sharpless, *Angew. Chem., Int. Ed.*, 2001, **40**, 2004–2021.

28 D. M. Eugene and S. M. Grayson, *Macromolecules*, 2008, **41**, 5082–5084.

29 D. Pasini, *Molecules*, 2013, **18**, 9512–9530.

30 X.-P. Qiu, F. Tanaka and F. M. Winnik, *Macromolecules*, 2007, **40**, 7069–7071.

31 Y. Satokawa, T. Shikata, F. Tanaka, X.-P. Qiu and F. M. Winnik, *Macromolecules*, 2009, **42**, 1400–1403.

32 Y.-Y. Yuan, J.-Z. Du and J. Wang, *Chem. Commun.*, 2012, **48**, 570–572.

33 R. Hoogenboom, F. Wiesbrock, H. Huang, M. A. Leenen, H. M. Thijs, S. F. van Nispen, M. van der Loop, C.-A. Fustin, A. M. Jonas and J.-F. Gohy, *Macromolecules*, 2006, **39**, 4719–4725.

34 A. Makino and S. Kobayashi, *J. Polym. Sci., Part A: Polym. Chem.*, 2010, **48**, 1251–1270.

35 J.-S. Park and K. Kataoka, *Macromolecules*, 2006, **39**, 6622–6630.

36 J.-H. Kim, E. Lee, J.-S. Park, K. Kataoka and W.-D. Jang, *Chem. Commun.*, 2012, **48**, 3662–3664.

37 J.-H. Kim, D. Yim and W.-D. Jang, *Chem. Commun.*, 2016, **52**, 4152–4155.

38 W. A. Velema, M. van der Toorn, W. Szymanski and B. L. Feringa, *J. Med. Chem.*, 2013, **56**, 4456–4464.

39 T. Ogoshi, K. Yoshikoshi, T. Aoki and T. A. Yamagishi, *Chem. Commun.*, 2013, **49**, 8785–8787.

40 M. Meyer and H. Schlaad, *Macromolecules*, 2006, **39**, 3967–3970.

41 J. Xu, J. Ye and S. Liu, *Macromolecules*, 2007, **40**, 9103–9110.